Int J Adv Manuf Technol (2016) 83:1441–1455
DOI 10.1007/s00170-015-7675-0

ORIGINAL ARTICLE

Experimental investigations, modeling, and optimization of multi-scan laser forming of AISI 304 stainless steel sheet

Kuntal Maji[1] · **D. K. Pratihar**[1] · **A. K. Nath**[1]

Received: 17 May 2012 / Accepted: 3 August 2015 / Published online: 14 August 2015

Abstract Laser forming experiments were conducted on AISI 304 stainless steel flat sheet to study the effects of process parameters and for developing an empirical model of bending angle, which could be useful to produce a class of developable surfaces from it using multiple parallel laser scans. Central composite design of experiments was used to perform the experiments, input–output relationships were established, and optimization of laser forming process under temperature gradient mechanism was carried out using a response surface methodology based on the experimental data. Laser power, scan speed, spot diameter, scan position, and number of scans were taken as input variables, and bending angle was considered as the output. The performance of the developed model was validated through a set of experimental data. The optimum process parameters for obtaining the maximum bending angle were determined, and those were verified through the real experiments. The effect of work-piece geometry on bending angle and that of multiple laser irradiations on bending rate were also investigated. Bending angle was found to be influenced by the work-piece geometry. Bending angle increased with the number of laser scans, but the bending rate decreased. Metallurgical changes at the laser irradiated zones of the laser formed samples, that is, micro-structures and micro-hardness were also studied using scanning electron microscope and Vickers' micro-hardness tester, respectively. Microstructures were found to be refined and micro-hardness of the bent zone got improved due to the laser forming.

Keywords Laser forming · Temperature gradient mechanism · Response surface methodology · Optimization · Geometric effect

✉ D. K. Pratihar
dkpra@mech.iitkgp.ernet.in

Kuntal Maji
kuntalmajiiitkgp@gmail.com

A. K. Nath
aknath@mech.iitkgp.ernet.in

[1] Department of Mechanical Engineering, Indian Institute of Technology Kharagpur, Kharagpur 721 302, India

1 Introduction

Laser forming is a complex thermo-mechanical process of forming sheets made of different materials, such as stainless steel, alloys of aluminum, titanium, and others. In this process, thermal energy of a controlled and defocused laser beam is used to induce plastic deformation to form the sheet metal. Laser forming has many advantages over the traditional sheet metal forming process. It requires no hard tooling or external forces, and there is no spring-back in this process. It depends on various process parameters, for example, laser power, scan speed, spot diameter, scan path and number of scans, thermo-physical properties and geometry of the work-piece material, and others. Depending on the combination of process parameters, mainly three types of mechanisms are operative in laser forming process and they are, namely temperature gradient mechanism (TGM), buckling mechanism (BM), and upsetting mechanism (UM). TGM develops a steep temperature gradient due to rapid heating of the surface. Compressive plastic strains are generated, when thermal expansion is hindered, causing bending towards the laser beam after cooling. BM is activated by the use of laser parameters, which do not develop much high temperature gradient along the thickness. The ratio of laser beam diameter to sheet thickness is relatively high compared to the case of TGM, which develops a large amount of thermo-elastic strain, and a local thermo-elastic-plastic

buckling of the material produces out of plane bending of the sheet. In the case of UM, the buckling is prevented by the relatively higher sheet thickness and an in-plane strain is produced.

Laser forming process depends on the complex interaction of various process parameters. The objective of this work was to study the effects of various process parameters and also that of material distribution around the laser irradiated zone on final deformation. This study also aimed to predict the bending angle for multiple scans to be useful to produce a class of developable surfaces from flat metal sheet and obtain the process parameters for achieving the maximum bending angle in multi-scan laser forming process.

2 Literature review

Several researchers carried out both theoretical and experimental investigations since the last two decades on different aspects of laser forming process to make it a feasible and economical process to be adapted by industries. However, the laser forming process has not achieved much attention from industries for large-scale applications due to a number of technology challenges realized by different investigators as discussed below.

Process modeling of laser forming is inevitable for its automation, and consequently, different models were developed in order to predict deformation using various techniques, such as analytical, numerical, empirical, and others [1]. Vollertsen [2] first developed a simple analytical model to determine bending angle in laser bending process using an energy approach. The model was built based on the assumption of elastic bending theory and did not consider the effect of spot diameter, and it could predict bending angles on the higher side. Later on, others proposed different models with improvement like Cheng and Lin [3], McBride et al. [4], Shen et al. [5], etc. Those models were developed based on simplified assumptions and were applicable to single scan only following straight path. They could become cumbersome to apply for multi-scans laser forming due to variations in absorptivity and other properties, and changing scan path positions. On the other hand, numerical models might be beneficial in such situations to calculate the bending angle and could give a better understanding of the transient nature of the process. Vollertsen et al. [6] first carried out numerical simulation of the laser bending process using finite element method (FEM) and finite difference method (FDM). Both temperature distributions and bending angle were determined from the simulations. Discretization was found to affect the temperature distribution only and FEM was found to give better results compared to the FDM to predict the bending angles. A number of numerical simulations of laser bending of different materials under different conditions were carried out by several researchers [7–10] to determine temperature distributions and deformation using the FEM. However, those models were found to take huge computational time particularly for multi-scan laser forming of large plates.

Some researchers also developed empirical models based on experimental data on multi-scan laser forming of different materials using various approaches. Yao et al. [11] investigated the laser bending of lead frame materials. They observed that the final bending angle increased with the laser power and number of laser scans, and decreased with the scan speed and holding time between two successive scans in multi-scan process. Experimental investigations were also carried out by various researchers [12–23] on multi-scan laser forming of different materials like carbon steel, mild steel, stainless steel, titanium alloys, etc., considering several process parameters, that is, both laser energy parameters and geometric parameters. Empirical models were also developed by them using different techniques, that is, response surface methodology, neural networks, etc. to laser form different simple 2D and 3D shapes. Laser forming of fiber metal laminate was investigated by Carey et al. [15] for multiple laser scans and found that both cumulative bending angle and bending rate per pass increased with the increase in laser power or decrease in scan speed. Birnbaum et al. [19] carried out both numerical and experimental investigations to study the effects of holding the work-piece, and laser scan position with respect to the clamped edge on its final deformation in laser forming process for both single and multiple laser scans. Average bending angle in case of clamped sample was found to be more than that of the unclamped case. Edwardson et al. [22] investigated and concluded that the bending rate decreased with the number of pass due to increase in incident area of laser spot and consequently, reduction of energy fluence because of component deformation. It has been felt from the past experimental research that deformation behavior of multi-scan laser forming is complex and to form a desired general 3D shape from flat sheet metal requires exhaustive experiments.

The effects of laser forming on mechanical and metallurgical properties of the formed components were investigated by several researchers [24–26] considering different materials and processing conditions. Controlling the properties of laser formed components in multi-scan laser forming process is challenging and very much important for their applications.

The effects of various process parameters on bending angle of different materials had been reported in the past through some theoretical and experimental studies. However, not much work had been carried out on the laser bending of metal sheets by considering the effects of multiple laser irradiations, material distributions around the laser irradiated region, and sheet geometry on bending deformation. Recently, response surface methodology (RSM) has been used by several researchers for modeling and optimization of various advanced

manufacturing processes [27, 28]. Understanding the deformation behavior and achieving desired properties of the laser formed parts in multi-scan laser forming are essential for its better implementation in industry.

The objective of this paper is to study the deformation behavior of the multi-scan laser bending of 304 stainless steel sheets through experiments and model the process using RSM. Experiments were conducted according to central composite design (CCD) to study the effects of different process parameters on the bending angle, which could be helpful to produce a class of developable surfaces using multiple parallel laser irradiations. Investigations were also carried out to study the effect of multiple laser irradiations on bending angle, bending rate, and the associated metallurgical changes. It is important to predict the deformation and properties of the laser formed components using multiple laser scans. Optimization was also carried out to determine the set of optimal process parameters for achieving the maximum bending angle.

The remaining part of this article has been organized as follows: Section 3 describes the experimental setup and explains the experimental procedure adopted in this study. Modeling and optimization methods used in the present work are described and the results are discussed in Section 4.1. The effects of Fourier number and sheet geometry are discussed in Section 4.2. Section 4.3 presents the effect of multiple laser scans on bending angle and bending rate with the associated metallurgical changes. Results of this study have been compared with that of the published literature in Section 4.4. Concluding remarks are made and the scopes for future study have been indicated in Section 5.

3 Experimental setup and procedure

Experiments were conducted on a fiber laser (wavelength= 1.07 μm, Model YLR-2000) having a maximum laser power of 2.0 kW (refer to Fig. 1). A 10-mm diameter collimated laser beam was delivered through an optical fiber onto a focusing optical system, which consisted of a lens of 200 mm focal length. This produced a minimum spot diameter of 250 μm at the focal plane. Nitrogen at 0.5 bar pressure was used as shielding gas for protecting the optical system. The work-pieces were AISI 304 stainless steel sheets of 120 mm× 40 mm×0.5 mm dimensions. The samples were cleaned using ethyl alcohol, and the zone to be laser irradiated was coated with permanent black ink to increase laser absorptivity. A 10, 000-W-Lp Ophir power meter was used to measure the average power, and the average absorption coefficients of the work-piece surfaces with and without the coating were found to be equal to 0.8 and 0.5, respectively. One end of the work-piece was held in a clamp and laser scans were performed

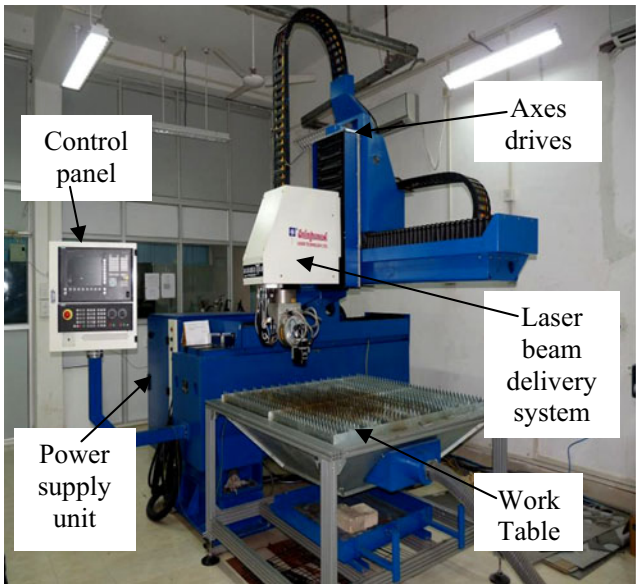

Fig. 1 Fiber laser system (2 kW)

parallel to the free edge of the samples, as shown in Fig. 2. In such straight line laser bending operation, bending angle is the angle made by the deformed portion of the sheet metal with the undeformed portion, as shown in Fig. 3.

Five inputs, namely laser power (p), scan speed (v), spot diameter (d), scan path position (r), and number of scans (n), were considered and bending angle (A) was taken as the output. Scan path position (r) is the non-dimensional distance measured from the free edge of the work-piece and calculated as the ratio of effective free length (EFL) to total free length (TFL). EFL and TFL are the distances measured from the free edge of the sheet to scan position and clamped end of the sample, respectively, as shown in Fig. 4. The

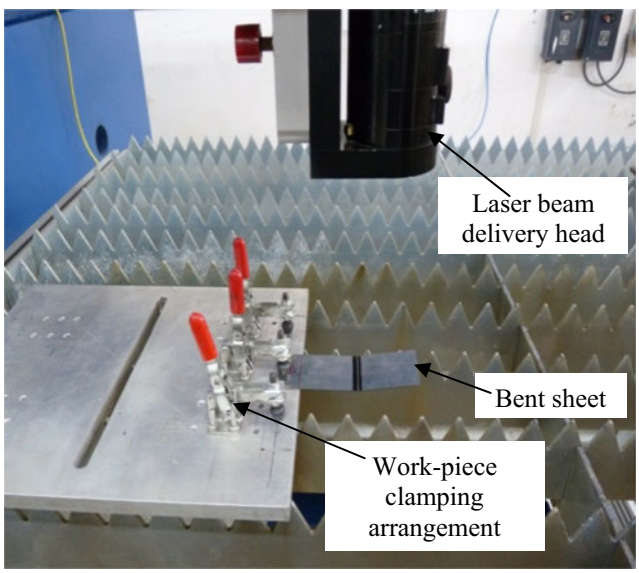

Fig. 2 Experimental setup

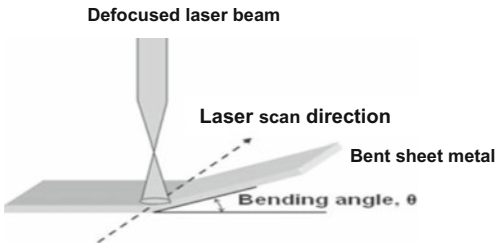

Fig. 3 Bending angle in laser bending operation

input process variables and their ranges considered in the study (refer to Table 1) were selected in a way to activate temperature gradient mechanism [29] of laser forming process. Experiments were carried out according to face centered central composite design of experiments [30, 31]. The deflection of the samples was measured using a laser displacement sensor attached to a 3-axes translational stage, as shown in Fig. 5. Deflections of the samples were measured at three to four locations along the scanning path direction and their average value was calculated. The bending angle was calculated by the triangulation method. An empirical model was developed based on the experimental data (refer to Table 4) for estimating the bending angle. The performance of the developed model was tested on some experimental data given in Table 5. Experiments were also performed to study the effect of Fourier number and work-piece dimensions on bending angle. The microstructure of the bent zone (both the laser irradiated zone and its cross-section) was studied by taking micrographs with a scanning electron microscope (SEM). Micro-hardness of the bent zone (both the top surface and the cross-section) was measured by a Vickers' microhardness tester using a 100 g applied load for 10 s duration.

4 Results and discussion

This section contains the results of statistical regression analysis used to establish input–output relationships of this process. Optimization was then carried out to determine the set of optimal process parameters corresponding to the maximum bending angle. The effects of Fourier number, work-piece dimensions, and multiple laser scans on bending angle were studied.

4.1 Statistical analysis

This section describes RSM-based modeling and optimization of the laser forming process using the experimental data collected according to the CCD.

4.1.1 Response surface methodology

RSM is a collection of mathematical and statistical techniques that are useful for the modeling and analysis of the problems, in which a response of interest is influenced by several variables and the objective is to optimize the response [30]. If all the independent variables are assumed to be measurable, then the response surface can be expressed as the following:

$$y = f(x_1, x_2, \ldots\ldots x_n) + \varepsilon \tag{1}$$

where $x_1, x_2, \ldots\ldots x_n$ are the independent variables and ε is the observed error or noise of the response y. RSM aims to determine a suitable approximation for the true functional relationship between the response and the independent variables. Generally a second-order polynomial in some ranges of the independent variables is used to develop an approximate model based on the experimental data obtained from the process or system. Multiple regression analysis is used for developing the types of empirical models required in the RSM, as given below.

$$y = \beta_0 + \sum_{i=1}^{k} \beta_i x_i + \sum_{i=1}^{k} \beta_{ii} x_i^2 + \sum_{i=1}^{k-1} \sum_{j=2}^{k} \beta_{ij} x_i x_j \,, \tag{2}$$

where β values are called the regression coefficients. The method of least square is used to determine the regression coefficients of Eq. (2).

4.1.2 Modeling of laser forming using response surface methodology

A second-order (quadratic) model was developed for the response, that is, bending angle using the RSM based on the

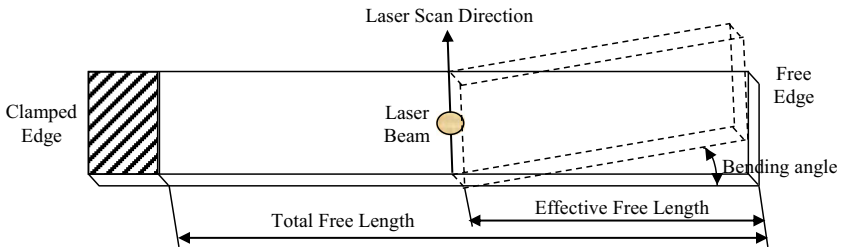

Fig. 4 Schematic view of the laser bending showing the experimental arrangement of sample and laser beam with effective free length (EFL) and total free length (TFL)

Table 1 Input variables and their ranges

SL. no.	Input variables	Uncoded symbol	Coded symbol	Minimum value	Mid-value	Maximum value
1	Laser power (W)	p	x_1	225	250	275
2	Scan speed (mm/s)	v	x_2	250.0	266.5	283.0
3	Spot diameter (mm)	d	x_3	0.500	0.625	0.750
4	Scan path position	r	x_4	0.25	0.50	0.75
5	Number of scans	n	x_5	5	10	15

collected experimental data as discussed above. Estimation of bending angle in multi-scan laser forming process using the developed model and verification of the model prediction are discussed below.

Estimation of the bending angle The bending angle in multi-scan laser bending process was modeled by carrying out an analysis using the Minitab 14 [32] software. The following expression was obtained for the bending angle in coded units:

$$\begin{aligned} A = {} & 9.08382 + 1.77147x_1 - 0.79520x_2 - 0.41980x_3 - 0.23137x_4 + 3.49431x_5 - 0.41930x_1^2 - 0.24930x_2^2 \\ & - 0.63097x_3^2 - 0.15763x_4^2 + 0.18903x_5^2 + 0.01688x_1x_2 + 0.55375x_1x_3 - 0.04521x_1x_4 + 0.69771x_1x_5 \\ & - 0.02167x_2x_3 - 0.03062x_2x_4 - 0.023188x_2x_5 + 0.02542x_3x_4 - 0.23292x_3x_5 + 0.20187x_4x_5 \end{aligned} \quad (3)$$

Regression coefficient of the developed model was found to be equal to 0.978, which indicates that the model is adequate enough to make further predictions. The significance test was carried out as given in Table 2. Here, the terms, such as Coef, SE Coef, T, and P, stand for the regression coefficient, standard error of estimated regression coefficient, value of the t test analysis, and probability value, respectively [30, 31]. Some of the terms were found to be insignificant, as their P values were more than 0.05, as the model was built at 95 % confidence level. However, those insignificant terms could not be removed from the model, as the lack of fit was seen to be significant as shown in the results of analysis of variance (ANOVA) presented in Table 3.

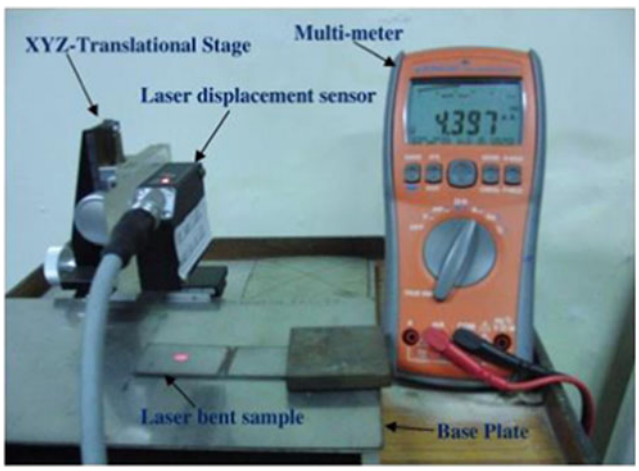

Fig. 5 Setup for measurement of bending angle

Table 2 Results of the significance test

Term	Coef	SE coef	T	P
Constant	9.08382	0.12892	70.460	0.000
x_1	1.77147	0.05982	29.612	0.000
x_2	−0.79520	0.05982	−13.292	0.000
x_3	−0.41980	0.05982	−7.017	0.000
x_4	−0.23137	0.05982	−3.868	0.000
x_5	3.49431	0.05982	58.411	0.000
x_1^2	−0.41930	0.22261	−1.884	0.062
x_2^2	−0.24930	0.22261	−1.120	0.265
x_3^2	−0.63097	0.22261	−2.834	0.005
x_4^2	−0.15763	0.22261	−0.708	0.480
x_5^2	0.18903	0.22261	0.849	0.398
x_1x_2	0.01688	0.06166	0.274	0.785
x_1x_3	0.55375	0.06166	8.980	0.000
x_1x_4	−0.04521	0.06166	−0.733	0.465
x_1x_5	0.69771	0.06166	11.315	0.000
x_2x_3	−0.02167	0.06166	−0.351	0.726
x_2x_4	−0.03062	0.06166	−0.497	0.620
x_2x_5	−0.23188	0.06166	−3.760	0.000
x_3x_4	0.02542	0.06166	0.412	0.681
x_3x_5	−0.23292	0.06166	−3.777	0.000
x_4x_5	0.20187	0.06166	3.274	0.001

Table 3 Results of ANOVA for bending angle

Source	*df*	Seq SS	Adj SS	Adj MS	*F*	*P*
Regression	20	1773.20	1773.20	88.660	242.88	0.000
Linear	5	1653.47	1653.47	330.693	905.92	0.000
Square	5	28.86	28.86	5.773	15.81	0.000
Interaction	10	90.87	90.87	9.087	24.89	0.000
Residual error	108	39.42	39.42	0.365		
Lack-of-fit	22	35.99	35.99	1.636	41.00	0.000
Pure error	86	3.43	3.43	0.040		
Total	128	1,812.63				

The terms used in Table 3, *df*, Seq SS, Adj SS, and Adj MS represent the degrees of freedom, sequential sum of square, adjusted sum of square and adjusted mean square, respectively [30, 31]. As the probability values (P) for the combined linear, square and interaction terms were found to be less than 0.05, it was concluded that they have significant contributions towards the bending angle. The F values for all the terms and lack of fit shown in Table 3 were found to be greater than F values of the standard statistical table, which were approximately 1.68, 2.31, 2.31, 1.93, and 1.70, respectively [31]. This also once again revealed that all the terms significantly influenced the bending angle and the lack of fit was also found to be significant. Thus, the insignificant terms could not be removed from the model. The bending angle can be expressed in terms of uncoded units of input variables, as given below.

$$\begin{aligned} A = {} & -90.8617 + 0.232447p + 0.468033v + 8.93851d + 3.26021r + 0.0534127n - 6.70880 \times 10^{-4}p^2 \\ & -9.15703 \times 10^{-4}v^2 - 40.3819d^2 - 2.52214r^2 + 0.00756133n^2 + 4.09091 \times 10^{-5}pv + 0.1772pd \\ & -0.00723333pr + 0.00558167pn - 0.0105051vd - 0.00742424vr - 0.00281061vn \\ & +0.813333dr - 0.372667dn + 0.1615rn \end{aligned} \tag{4}$$

Effects of process parameters on bending angle The effects of the process parameters (Table 4) were studied through surface plots for the bending angle with all five input variables, as shown in Fig. 6. The bending angle was found to increase with the increase in laser power (p) and number of scans (n), but decreased with the increase of scan speed (v). It happened so, because in all the cases, line energy input per unit length (p/v) increases. However, there is an optimum value of spot diameter (d) and scan path position (r) for the maximum value of bending angle, as it was found to first increase and then decrease. The amount of deformation in thermal metal forming varies with the size of the plastic zone and energy density. For smaller spot diameter, the size of the plastic zone is small, even though the energy density is high. When the spot diameter increases, the size of the plastic zone increases and so the bending angle. However, when there is a further increase in spot diameter, bending angle decreases, as the energy density decreases. This variation of bending angle with the spot diameter could be further explained by considering radial heat loss during the laser forming process. The rise in surface temperature in 1D heat conduction during laser material processing [33] can be given by the Eq. (5).

$$\Delta T = \frac{2Ap}{K\pi a^2}\sqrt{\frac{k\,2a}{v}}\cdot\left\{\frac{1}{\sqrt{\pi}} - ierfc\,\frac{a}{2\sqrt{k\,2a/v}}\right\} \tag{5}$$

where A, p, a, v, K, and k are the absorptivity, laser power, beam radius at the surface, scan speed, thermal conductivity, and thermal diffusivity, respectively. The bending angle, $\propto_b$ can be expressed as the following, considering the simplified analytical model [2].

$$\propto_b = \frac{3l_h \propto_{th} \Delta T}{2s_0} = \frac{3a \propto_{th} \Delta T}{s_0} \tag{6}$$

where spot radius is $a = l_h/2$, l_h is the width of the heated region, $\propto_{th}$ is the coefficient of thermal expansion, ΔT is the temperature rise in the heated zone, and s_0 is the sheet thickness. By substituting the value of ΔT from Eq. (5) in Eq. (6), the expression for the bending angle was obtained as follows:

$$\propto_b = \frac{6\sqrt{2k} \propto_{th} Ap}{Ks_0\pi\sqrt{\pi}} \frac{1}{\sqrt{av}} \left\{1 - \sqrt{\pi}\, ierfc\,\frac{\sqrt{av}}{2\sqrt{2k}}\right\} \tag{7}$$

This expression shows that for a large value of a, the terms: $(ierfc\,\frac{\sqrt{av}}{2\sqrt{2k}}) \rightarrow 0$ and $\propto_b \propto \frac{1}{\sqrt{a}}$, when other parameters are kept constant. However, as a is reduced, the term: $\left\{1 - \sqrt{\pi}\, ierfc\,\frac{\sqrt{av}}{2\sqrt{2k}}\right\}$ reduces and $\frac{1}{\sqrt{a}}$ term increases. Therefore, there is an optimum value of a for which the bending angle ($\propto_b$) will be the maximum. There was also an optimum scan path position for the maximum bending angle and it was found near the middle of the work-piece as shown in

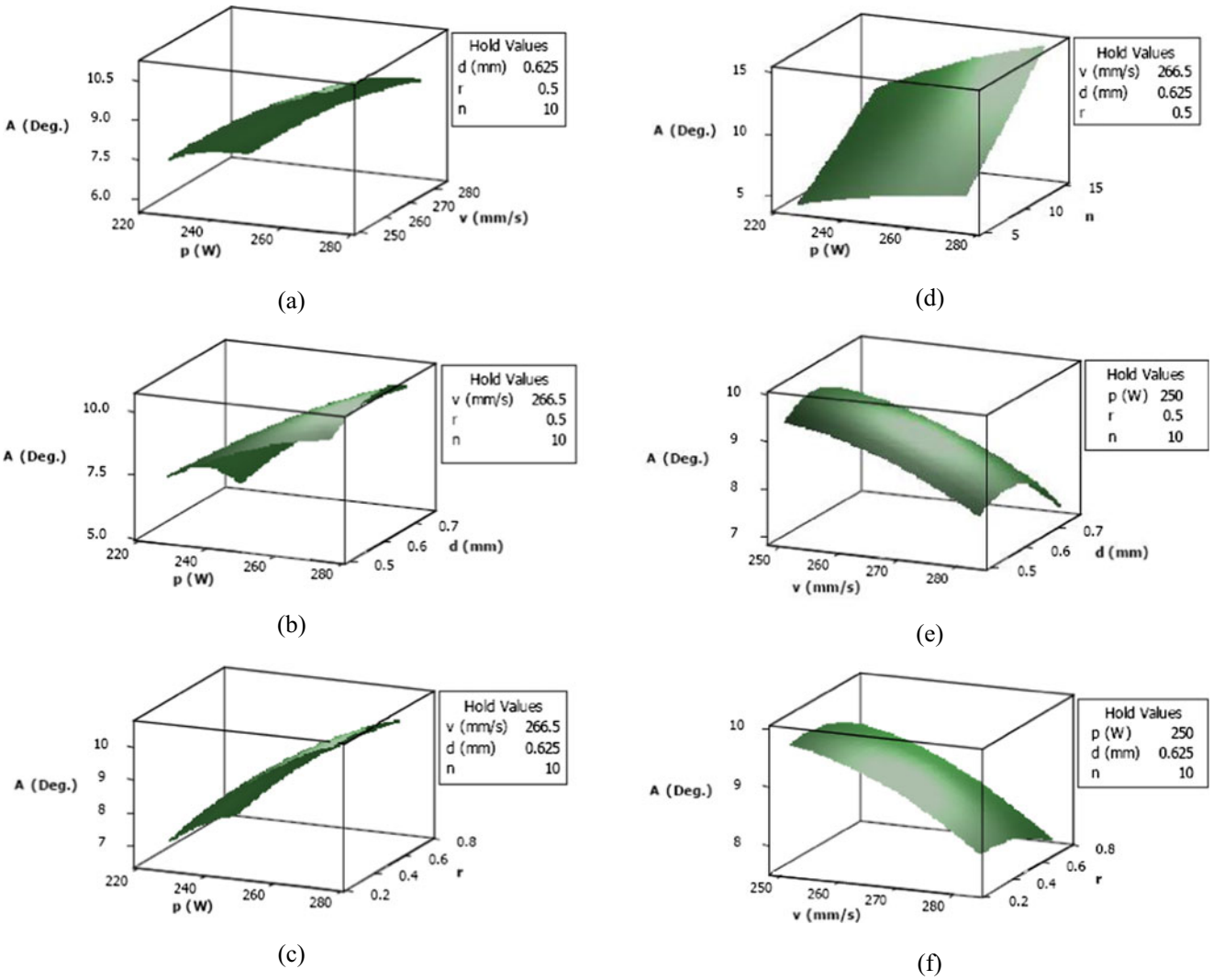

Fig. 6 Surface plots of bending angle (*A*) for different combinations of input variables

Fig. 6. Similar results were also reported by other investigators [34–36]. This was mainly due to the influence of variation of the mechanical constraint provided by the surrounding cold material around the laser irradiated zone, as the thermal field remains unchanged over the time during which deformations occur, and also because of the difficulty involved in bending the sheet near to the free and clamped edges compared to the middle of the sheet. As the scan position approached the edges of the sample, the mechanical restraining force decreased. This is due to the fact that the laser heated material adjacent to both the edges of the work-piece can expand more freely because of the less volume of material providing relatively lower rigid surrounding compared to that at the middle of the work-piece. Moreover, bending angle depends on the plastic strain and compressive stress along the transverse direction of the scan path, which are found to be the maximum near the middle of the sheet and decrease towards the edges of the sample. Therefore, the maximum bending angle is achieved near the middle of the sheet. Similar results for the scan path position were also achieved by optimizing the process for maximum bending angle and verified experimentally, as detailed in Section 4.1.3.

Verification of the developed model The estimation of bending angle in multi-scan laser bending using the developed RSM model was tested through a separate set of experimental data. The developed model for bending angle was verified with 15 experimental test data (refer to Table 5), and its prediction accuracy was found to be satisfactory. The experimental and predicted bending angles are shown in Fig. 7. The value of average absolute percent deviation in predictions of bending angles was found to be equal to 7.82.

4.1.3 Optimization of bending angle using desirability function approach

The response, namely bending angle, was optimized using desirability function approach [30, 31, 37] with the help of

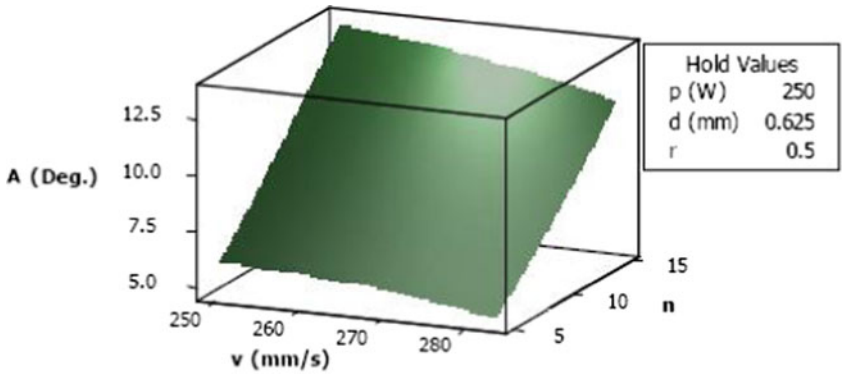

(g)

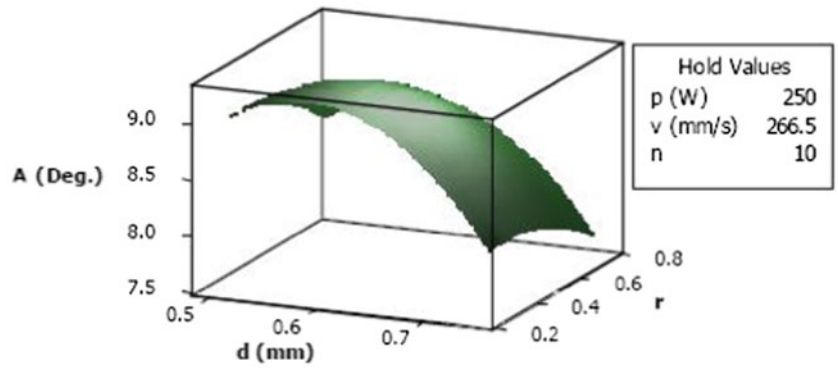

(h)

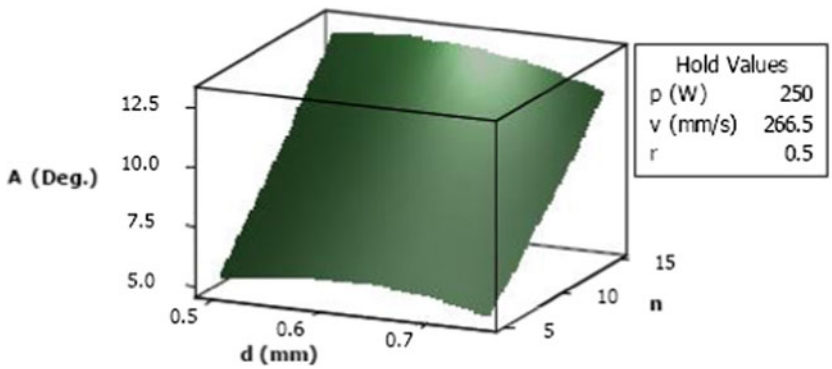

(i)

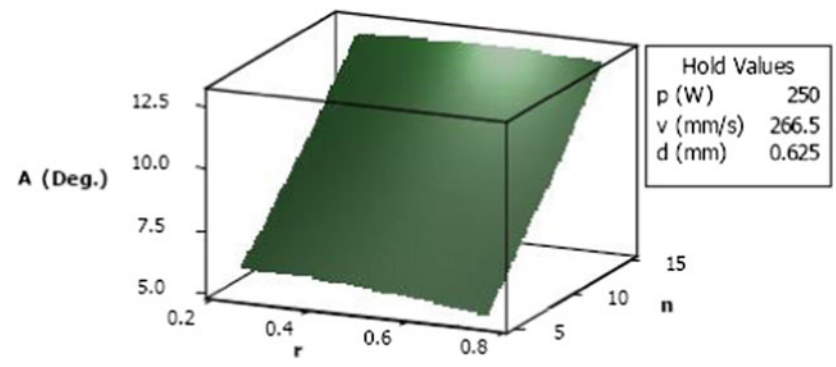

(j)

Fig. 6 (continued)

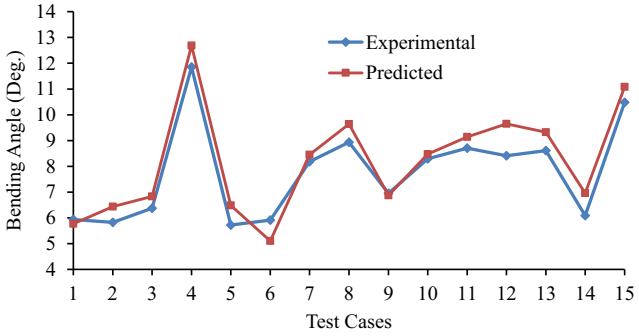

Fig. 7 Comparison of experimental and RSM model predicted bending angles

response optimizer in Minitab 14 software. The desirability function involves transformation of the response variable $f(x_i)$ to a desirability value D, where $0 \le D \le 1$ and x_i are the input variables. The value of D increases as the desirability of the response increases. A desirability function of $f(x_i)$, $D(f(x_i))$ lying within a range of (0, 1) can be produced using the following transformation [36]:

$$D(f(x_i)) = \begin{cases} 0, & if \quad f(x_i) \le f_{min} \\ \left(\frac{f - f_{min}}{f_{max} - f_{min}}\right)^r, & if \quad f_{min} \le f(x_i) \le f_{max} \\ 1, & if \quad f(x_i) \ge f_{max} \end{cases}$$

The shape of the desirability function depends on the value of the weight indicated by "r." The value of r may vary from 0.1 to 10. To maximize a response, it is required to set a target value and an allowable minimum response value. The desirability for this response above the target value is one and below the minimum acceptable value, the desirability is zero. The closer the response to the target, the closer the desirability is to one. Finally, Minitab employs a reduced gradient algorithm with multiple starting points that maximizes the desirability to determine the optimal solution.

Bending angle was found to vary from 1.66° to 15.38° in the set of experimental data collected according to the CCD (refer to Table 4). To maximize the bending angle (A), the target was set at 16° and the lower value was taken as 1.5° with a weight of 0.1 for the desirability function and importance value of 10 for the response. The above values of the lower bound, target and weight of the desirability function were decided after trying with their different values within the range of the experimental data and that of the weight values of the desirability function. The importance value varies from 0.1 to 10 to emphasis on a particular response and its value was taken to be equal to 10, as only one response was considered. The maximum bending angle was found to be equal to 15.5835° with a desirability value of D=0.99709, and the corresponding set of input parameters was as follows: p= 275.0 W, v=250.0 m/s, d=0.6 mm, r=0.4636, and n=15. The value of scan path position for the maximum bending angle was seen to be equal to 0.4636, which is near to 0.5, as reported by Yu et al. [34]. The optimum value of this bending angle was validated through the experimental data. Experiment was conducted with the above set of optimal inputs but the value of scan path position was taken as 0.46 instead of 0.4636, and the corresponding optimum bending angle was found to be equal to 16.85°.

4.2 Effects of fourier number and work-piece dimensions on bending angle

The effects of Fourier number and sheet geometry or work-piece dimensions on bending angle were also investigated. Fourier number or Fourier modulus is a non-dimensional parameter that characterizes transient heat conduction and is defined as $\frac{\propto t}{R^2}$, where $\propto$ is the thermal diffusivity (m^2/s), t is the characteristic time (s), and R is the length (m) through which heat conduction occurs. For laser forming process, characteristic time t is calculated as d/v, where d is the laser spot diameter and v is the scan speed, and R is the sheet thickness. Therefore, the modified Fourier number can be expressed as $F'_O = \frac{\propto d}{s^2 v}$, where s is the sheet thickness. For temperature gradient mechanism, steep temperature gradient along the thickness direction is to be produced by laser scanning and the value of F' should be low (F' <<1) [29]. In the previous section, it had been presented that the bending angle decreases with the increase of scan speed because the line energy (p/v) decreases for the fixed values of all other process parameters. However, if scan speed is increased keeping the line energy constant, Fourier number reduces, and consequently, the bending angle increases. The temperature gradient along the thickness direction increases with the decrease in Fourier number due to an increase of scan speed. The variation of bending angle with Fourier number had been shown in Fig. 8 for two different spot diameters and sheet thickness values after maintaining the line energy (p/v) constant separately.

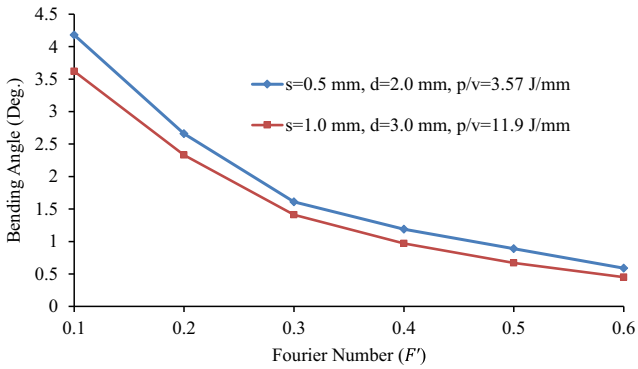

Fig. 8 Effect of Fourier number (F') on bending angle (A)

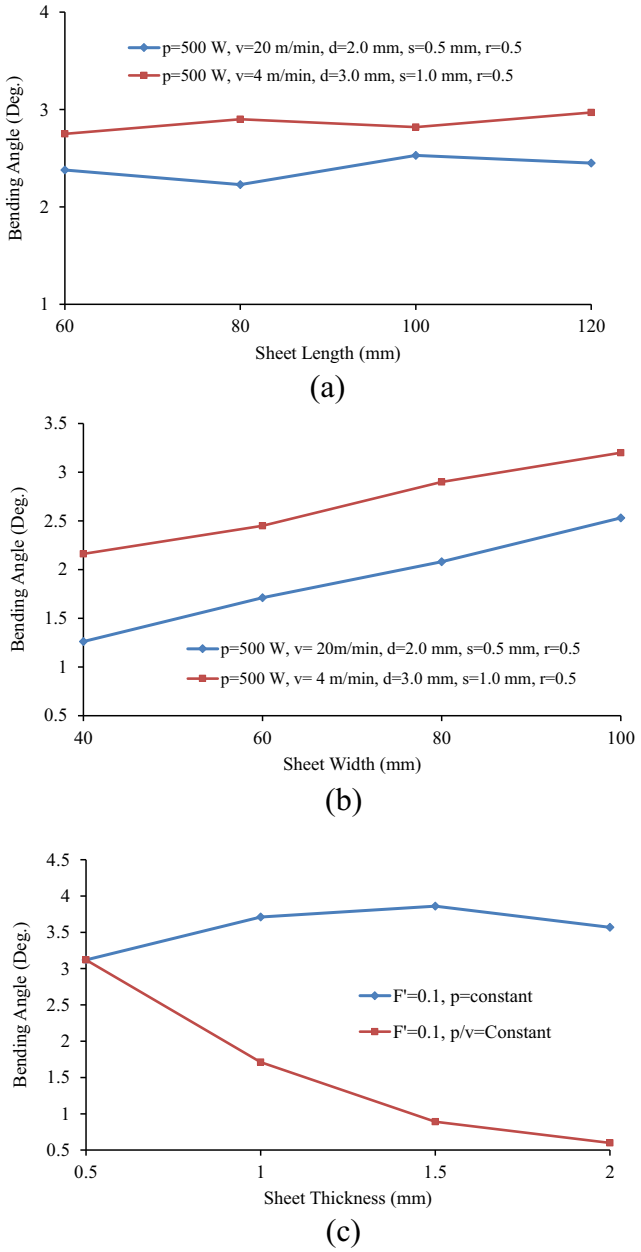

Fig. 9 Effect of sheet length (*l*), width (*w*), and thickness (*s*) on bending angle (*A*)

The effect of work-piece dimensions, that is, sheet length on bending angle was also studied. Figure 9a, b, c shows the variations of the bending angle with the length (transverse to the laser scan) of work-piece, its width (along the laser scan) and thickness, respectively. Experiments were performed for two typical sets of process parameters and two different sheet thicknesses (0.5 and 1.0 mm). Sheet length was found to have a little effect on the bending angle, (refer to Fig. 9 (a)). However, bending angle increased with the increase of work-piece width or scan length, as shown in Fig. 9 (b). Similar trend was also reported by Shi et al. [20]. As the work-piece width increased, the amount of cold material of both the heated and unheated zones increased, which could provide a higher restraining force to prevent thermal expansion of the heated zone. This resulted into the larger compressive force and plastic strain, which could lead to increase in bending angle. Increase of bending angle with the width could also be attributed to the pre-bending and post-bending effects [35]. For the constant Fourier number and line energy, bending angle decreased with the increase of sheet thickness. This is because of the fact that the bending moment required to bend thicker sheet increases and provides more restriction against deformation. However, when Fourier number and power were kept constant and the thickness was increased, bending angle initially increased and then showed a decreasing trend (refer to Fig. 6 (c)). It happened so, because the bending angle was increased due to an increase in line energy, but when the line energy was too high, melting took place and the bending angle was reduced, as shown in Fig. 9 (c). Fourier number was maintained at constant value for the increasing sheet thickness by reducing the scan speed (as $F' = \frac{\alpha d}{s^2 v}$ and $v \propto 1/s^2$). This resulted in an increase in line energy at constant laser power and thereby, increased the bending angle as well. Beyond a certain thickness, the scan speed became so low that onset of surface melting sets in causing reduction in flow strength of the material. It had been reported that beyond a certain saturation temperature T_{sat}, the plastic strain and therefore, bending angle tends to saturate [4]. With the lowering of flow strength and increase of thermal stress, the material could flow out of plane causing increase in thickness. This could restrict the bending angle at higher line energy beyond a certain limit.

4.3 Effect of multiple laser scans on bending angle and bending rate

The bending angle (cumulative) was found to increase with the number of scans along the same laser irradiation track; however, the average bending angle (per scan) or the bending rate tended to decrease, as shown in Fig. 10. Experiments were carried out for two different sets of process parameters and in both the cases similar trends were found. However, the increase of bending angle and reduction of bending rate was found to be more significant in case of larger ratio of spot diameter to sheet thickness keeping the energy density constant. Reduction in average bending angle or bending rate with the number of scans could be due to a number of reasons, such as strain hardening, section thickening, absorptivity variation, thermal, and geometric effects due to multiple laser irradiations [21–23].

- Strain hardening and metallurgical changes
- In laser forming, material gets plastically deformed due to the laser induced thermal stress and each laser scan

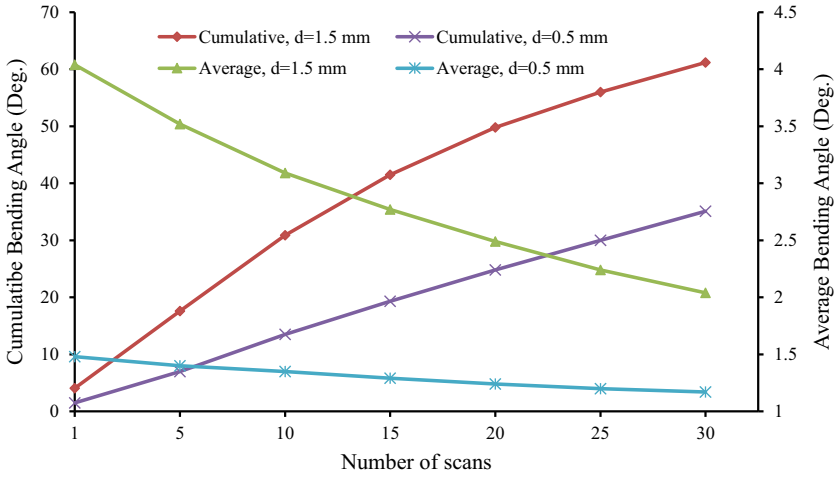

Fig. 10 Effect of multiple scans on bending angle and bending rate in laser forming process

produces some bending in the sheet and thus, increases the dislocation density [38]. As a result, the sheet metal gets strain hardened, which increases the strength and hardness of the laser formed material, resulting in the decrease in average bending angle. The microhardness measurement of the bent samples corroborates this effect. In multiple laser scans, though surface melting was avoided by proper selection of the process parameters, some modifications in the microstructures of the laser irradiated surface were observed, as shown in Fig. 11a, b for single and fifteen scans, respectively. Figure 12a, b shows the microhardness distributions of the bent zones, that is, along the transverse direction of the laser scan and thickness of the sheet, respectively. This increase in microhardness at the laser irradiated zone could be attributed to the strain hardening and also to the formation of refined grained microstructure due to rapid heating and quenching [24].

- Section thickening
- During laser forming, as the temperature at the top surface increases, the thermal stress increases until the local yield stress of the material is reached [4]. Under the compressive stress imposed by the surrounding material, the laser-heated material then flows in a direction normal to the constraint in the thickening of the laser irradiated region. This increase in thickness (t) reduces the volume energy ($\frac{p}{vdt}$) [18] for the same laser power (p), spot diameter (d), and scan speed (v) and also increases the required bending moment. These factors would cause a decrease in average bending angle per scan.
- Geometric effects
- During laser forming, as the bending angle increases, the area irradiated with the laser beam increases, resulting in reduced energy density. This would also reduce the bending per scan with the increasing number of scans [22].
- Absorptivity variation
- The absorptivity of the surface tends to be reduced with the number of laser scans because the absorptive coatings (permanent black ink used for the experiments) are deteriorated with repeated laser irradiations. The decrease in average bending angle per scan with the increasing number of scans could also be partly attributed to this effect.
- Thermal effects
- Since the bending angle depends on the temperature gradient, the decrease in bending rate in multi-scan laser forming process can be attributed to the dwell time or holding time between the successive passes [39], and also

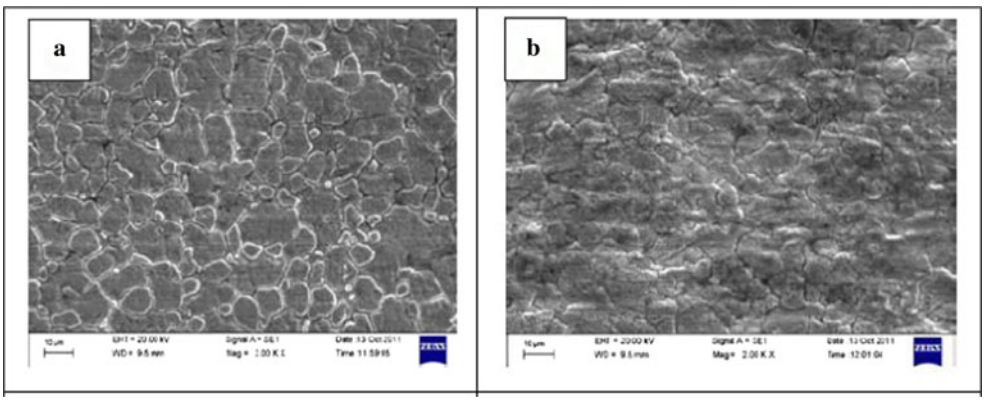

Fig. 11 Microstructures of laser irradiated surface for **a** single and **b** 15 laser scan(s)

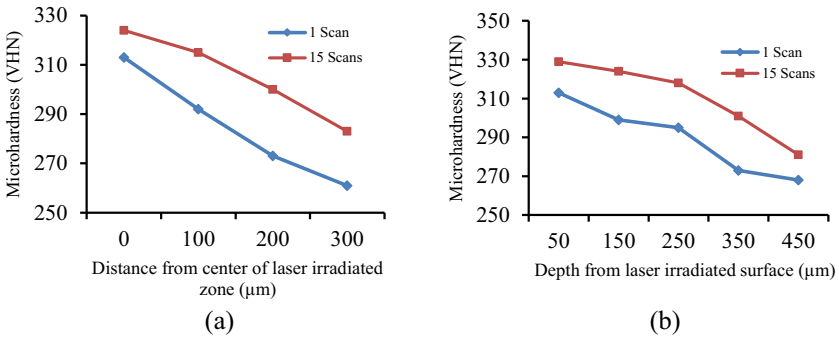

Fig. 12 Variations of micro-hardness **a** from the center of the laser irradiated zone in the transverse direction and **b** along the depth of the sheet

the cooling condition. By providing adequate holding time between two scans, this reduction in bending rate may be avoided. However, it increases the forming time, which can also be reduced by forced cooling, as reported by Cheng and Yao [21].

The factors influence the bending rate in a complex manner and one or more factors may be more dominant than the others.

4.4 Comparison with other researchers' work

This section presents the comparison of results of this study with other researchers' work. In this work, bending angle was found to increase with the increase in laser power and number of laser scans, and it was seen to decrease with the increase in scan speed. However, it was found to have optimum values for both laser spot diameter and scan position for the maximum bending angle within operating window of the process parameters considered for laser bending of AISI304 stainless steel. Yao et al. [11] obtained similar trends for laser power, scan speed and number of laser scans in laser bending of lead frame materials. Shichun and Jinsong [12] found similar results for all laser parameters except spot diameter for steel and aluminum alloy sheet. Bending angle was found to decrease with the increase of spot diameter and in this article, it was found to have an optimum value as explained in Section 4.1.2. Among the sheet geometric parameters, sheet length was found to have insignificant effect on bending angle and it was found to increase with sheet width and decrease with sheet thickness. Shichun and Jinsong [12] observed sheet thickness to be the significant influencing factor only. Shi et al. [20] found similar trends with the present study except the decreasing nature of bending angle with sheet length for DC01 steel. Results of Birnbaum et al. [19] and Jha et al. [36] obtained for low carbon steel (AISI1010) and stainless steel (AISI304) sheets, respectively, in terms of laser scan position, were seen to be similar to that of the present study. Marya and Edwards [14] and Edwardson et al. [23] obtained the similar trends for bending angle and bending rate with the number of laser scans in multi-scan laser bending of different materials like mild steel, titanium and aluminum alloys etc. Metallurgical changes of laser formed components in multi-scan laser forming presented in this study were also similar to that reported by Majumdar et al. [24] and Walczak [25] for stainless steel sheets of grades 304 and 302, respectively.

5 Conclusions and future scope

Response surface methodology was able to predict bending angles within the ranges of the input variables considered with a reasonable accuracy in laser forming process. Analysis of variance identified that all the input variables, that is, laser power, scan speed, spot diameter, scan position and number of scans significantly influence the bending angle.

The following conclusions were made:

- Bending angle increased with laser power and number of scans but decrease with scan speed.
- There were optimum values for both spot diameter and scan path position for the maximum bending angle.
- Though the total bending angle increased with the number of scans, the bending rate decreased and this effect was more significant in case of larger laser irradiated area and for constant energy density.
- Among the sheet geometric parameters, bending was found to be influenced by sheet thickness and width and was independent of sheet length.
- Bending angle increased with the decrease in modified Fourier number.
- Microstructures of the laser formed samples at the laser irradiated bent zone was refined and micro-hardness of the bent zone increased compared to that of the base metal.

The model was developed for the straight scan paths parallel to the free edge of the sheet, which could be used to produce a class of developable surfaces. However, this idea can be extended to other 2D and 3D laser forming processes considering laser scans in different orientations using both the mechanisms of laser forming, that is, TGM and UM.

Appendix

Table 4 Experimental data collected according to CCD to develop the model of bending angle

SL. no.	Input parameters					Output: bending angle (Deg.)		
	p (W)	v (mm/s)	d (mm)	r	n	A_1	A_2	A_3
1	225	250.0	0.500	0.25	5	4.81	5.34	5.07
2	275	250.0	0.500	0.25	5	6.71	6.61	6.82
3	225	283.0	0.500	0.25	5	4.06	4.52	3.76
4	275	283.0	0.500	0.25	5	4.56	4.20	5.00
5	225	250.0	0.750	0.25	5	3.97	3.74	3.55
6	275	250.0	0.750	0.25	5	5.69	5.85	6.04
7	225	283.0	0.750	0.25	5	2.14	1.95	2.18
8	275	283.0	0.750	0.25	5	6.45	6.29	6.68
9	225	250.0	0.500	0.75	5	4.12	4.21	4.19
10	275	250.0	0.500	0.75	5	4.41	4.73	4.56
11	225	283.0	0.500	0.75	5	2.22	2.27	2.17
12	275	283.0	0.500	0.75	5	5.05	4.95	5.00
13	225	250.0	0.750	0.75	5	3.56	3.63	3.73
14	275	250.0	0.750	0.75	5	6.12	6.23	5.94
15	225	283.0	0.750	0.75	5	1.74	1.58	1.66
16	275	283.0	0.750	0.75	5	3.89	4.08	4.20
17	225	250.0	0.500	0.25	15	11.30	11.50	11.06
18	275	250.0	0.500	0.25	15	15.21	14.47	14.83
19	225	283.0	0.500	0.25	15	8.58	8.65	8.79
20	275	283.0	0.500	0.25	15	13.00	12.40	12.80
21	225	250.0	0.750	0.25	15	8.07	8.28	7.90
22	275	250.0	0.750	0.25	15	15.47	15.28	15.40
23	225	283.0	0.750	0.25	15	7.16	7.21	7.26
24	275	283.0	0.750	0.25	15	12.24	12.47	11.93
25	225	250.0	0.500	0.75	15	11.70	11.06	11.25
26	275	250.0	0.500	0.75	15	14.20	14.34	14.47
27	225	283.0	0.500	0.75	15	9.48	9.54	9.36
28	275	283.0	0.500	0.75	15	12.53	12.46	12.5
29	225	250.0	0.750	0.75	15	7.98	8.09	8.28
30	275	250.0	0.750	0.75	15	15.20	15.28	15.10
31	225	283.0	0.750	0.75	15	6.46	6.30	6.38
32	275	283.0	0.750	0.75	15	12.25	12.31	12.37
33	225	266.5	0.625	0.50	10	6.33	6.45	6.21
34	275	266.5	0.625	0.50	10	11.13	10.84	10.95
35	250	250.0	0.625	0.50	10	8.87	8.95	9.04
36	250	283.0	0.625	0.50	10	8.67	8.84	8.56
37	250	266.5	0.500	0.50	10	9.30	8.78	9.02
38	250	266.5	0.750	0.50	10	7.44	7.75	8.35
39	250	266.5	0.625	0.25	10	8.88	9.00	8.60
40	250	266.5	0625	0.75	10	9.25	8.78	8.97
41	250	266.5	0.625	0.50	5	4.60	4.85	5.08
42	250	266.5	0.625	0.50	15	13.67	13.80	13.56
43	250	266.5	0.625	0.50	10	9.24	9.13	9.19

Table 5 Data collected for testing the model of bending angle

SL. no.	Input parameters					Bending angle (degree)		% deviation in prediction
	p (w)	v (mm/s)	d (mm)	r	n	Experimental (A_e)	Predicted (A_p)	
1	230	258.33	0.550	0.30	6	5.93	5.77	2.62
2	270	275.00	0.700	0.60	6	5.82	6.43	10.54
3	240	275.00	0.550	0.40	8	6.37	6.83	7.29
4	260	258.33	0.700	0.70	14	11.85	12.69	7.07
5	240	258.33	0.700	0.70	8	5.72	6.48	13.31
6	230	275.00	0.550	0.40	6	5.91	5.10	13.73
7	270	258.33	0.550	0.60	8	8.18	8.45	3.35
8	240	275.00	0.700	0.30	14	8.93	9.64	7.92
9	270	275.00	0.700	0.30	6	6.95	6.87	1.10
10	260	258.33	0.550	0.40	8	8.29	8.47	2.12
11	230	258.33	0.550	0.70	12	8.70	9.14	5.01
12	240	275.00	0.700	0.60	14	8.41	9.65	14.75
13	230	258.33	0.550	0.30	12	8.61	9.32	8.24
14	260	258.33	0.700	0.40	6	6.08	6.96	14.54
15	270	275.00	0.550	0.60	12	10.48	11.08	5.69

References

1. Shen H, Vollertsen F (2009) Modeling of laser forming—an review. Comput Mater Sci 46:834–840
2. Vollertsen F (1994) An analytical model for laser bending. Lasers Eng 2:261–276
3. Cheng PJ, Lin SC (2001) An analytical model to estimate angle formed by laser. J Mater Process Technol 108:314–319
4. McBride R, Bardin F, Gross M, Hand DP, Jones JDC, Moore AJ (2005) Modeling and calibration of bending strains for iterative laser forming. J Phys D Appl Phys 38:4027–4036
5. Shen H, Shi Y, Yao Z, Hu J (2006) An analytical model for estimating deformation in laser forming. Comput Mater Sci 37:593–598
6. Vollertsen F, Geiger M, Li WM (1993) FDM and FEM simulation of laser forming: a comparative study. Proceeding of the Fourth International Conference on Technology of Plasticity, 1793–1798
7. Kyrsanidi AK, Kermanidis TB, Pantelakis SG (1999) Numerical and experimental investigation of the laser forming process. J Mater Process Technol 87:281–290
8. Zhang L, Michaleris P (2004) Investigation of Lagrangian and Eulerian finite element methods for modeling the laser forming process. Finite Elem Anal Des 40:383–405
9. Griffiths J, Edwardson SP, Dearden G, Watkins KG (2010) Finite element modeling of laser forming at macro and micro scales. Phys Procedia 5:371–380
10. Hu J, Dang D, Shen H, Zhang Z (2012) A finite element model using multi-layered shell element in laser forming. Opt Laser Technol 44:1148–1155
11. Yao CL, Chan KC, Lee WB (1998) Laser bending of lead frame materials. J Mater Process Technol 82:117–121
12. Shichun W, Jinsong J (2001) An experimental study of laser bending for sheet metals. J Mater Process Technol 110:160–163
13. Li W, Yao YL (2001) Laser forming with constant line energy. Int J Adv Manuf Technol 17:196–203
14. Marya M, Edwards GR (2001) A study on the laser forming of near-alpha and metastable beta titanium alloy sheets. J Mater Process Technol 108:376–383
15. Carey C, Cantwell WJ, Dearden G, Edwards KR, Edwardson SP, Watkins KG (2010) Towards a rapid, non-contact shaping method for fiber metal laminates using a laser source. Int J Adv Manuf Technol 47:557–565
16. Pennuto J, Choi J (2005) Characteristics of parallel irradiations in laser forming of stainless steel. J Laser Appl 17(4):235–242
17. Liu C, Yao YL (2002) Optimal and robust design of the laser forming process. J Manuf Process 4:52–66
18. Cheng PJ, Lin SC (2000) Using neural networks to predict bending angle of sheet metal formed by laser. Int J Mach Tools Manuf 40:1185–1197
19. Birnbaum AJ, Cheng P, Yao YL (2007) Effects of clamping on the laser forming process. J Manuf Sci Eng 129:1035–1044
20. Shi Y, Hu J, Dong C (2011) Analysis of the geometric effect on the forming accuracy in laser forming. Proceedings of the Institution of Mechanical Engineers, Part B: J Eng Manuf 225:1792–1800
21. Cheng J, Yao YL (2001) Cooling effects in multi-scan laser forming. J Manuf Process 3:60–72
22. Edwardson SP, Abed E, Bartkowiak K, Dearden G, Watkins KG (2006) Geometric influences on multi-pass forming. J Phys D Appl Phys 39:382–389
23. Edwardson SP, Griffiths J, Dearden G, Watkins KG (2010) Temperature gradient mechanism: overview of the multiple pass controlling factors. Phys Procedia 5:53–63
24. Majumdar JD, Nath AK, Manna I (2004) Studies on laser bending of stainless steel. Mater Sci Eng A 385:113–122
25. Walczak M, Grez JR, Celentano D, Lima EBF (2010) Sensitization of AISI 302 stainless steel during low-power laser forming. Opt Lasers Eng 48:906–914
26. Knupfer SM, Paradowska AM, Kirstein O, Moore AJ (2012) Characterization of the residual strains in iterative laser forming. J Mater Process Technol 212:90–99
27. Maji K, Pratihar DK (2011) Modeling of electrical discharge machining process using conventional regression analysis and genetic algorithms. J Mater Eng Perform 20:1121–1127
28. Sun Y, Hao M (2012) Statistical analysis and optimization of process parameters in Ti6Al4V laser cladding using Nd:YAG laser. Opt Lasers Eng 50:985–995

29. Steen WM, Mazumder J (2010) Laser material processing, 4th edn. Springer, London
30. Montgomery DC (2001) Design and analysis of experiments. Wiley, New York
31. Dean A, Voss D (2006) Design and analysis of experiments. Springer (India), New Delhi
32. Minitab Inc. (2004) Minitab 14, Statistical Software. http://www.minitab.com
33. Dowden JM (2001) The mathematics of thermal modeling: an introduction to the theory of laser materials processing. Chapman and Hall CRC Press, Florida
34. Yu G, Masubuchi K, Maekawa T, Patrikalakis NM (2001) FEM simulation of laser forming of metal plates. J Manuf Sci Eng 123: 405–410
35. Cheng P, Yao YL, Liu C, Pratt D, Fan Y (2005) Analysis and prediction of size effect on laser forming of sheet metal. J Manuf Process 7:28–41
36. Jha GC, Nath AK, Roy SK (2008) Study of edge effect and multi-curvature in laser bending of AISI 304 stainless steel. J Mater Process Technol 197:434–438
37. Derringer G, Suich R (1980) Simultaneous optimization of several response variables. J Qual Technol 12(4):214–219
38. Dieter GE (1986) Mechanical metallurgy, 3rd edn. Mc Graw-Hill, New York
39. Bartkowiak K, Dearden G, Edwardson SP, Watkins K (2004) Development of 2D and 3D forming strategies for thin section materials using scanning optics. Proc. of ICALEO Laser Institute of America, Orlando